Oxygen Reduction Reaction on Pt/C Electrocatalysts Obtained by a Photo-Chemical Route

R. G. González Huerta[1], M. A. Valenzuela[1], O. Martínez-Álvarez [2], H. H. Rodríguez[2], B. Ruiz-Camacho[1,2*,]

[1]ESIQIE-IPN, Laboratorio de Catálisis, UPALM, CP 07738, México D.F
[2]Ingeniería en Energía, Universidad Politécnica de Guanajuato, Av. Universidad Norte s/n, Juan Alonso Cortazar Guanajuato, C.P. 38438, México.

ABSTRACT

Platinum nanoparticles with homogeneous dispersion on carbon Vulcan was obtained at room temperature by irradiation of an alcoholic solution of $C_{10}H_{14}O_4Pt$ with UV-light. The electrocatalyst were characterized by X-ray diffraction and transmission electronic microscopy techniques. TEM micrographs and XRD results confirmed the formation of platinum nanoparticles (4 nm) with a high dispersion onto the carbon. The electrochemical active surface area was determinate by CO stripping and hydrogen-adsorption/desorption reactions. The electrochemical activity and stability of Pt/C for the oxygen reduction reaction (ORR) were determined by rotating disk electrode (RDE) at different temperatures. An apparent enthalpy of activation $\Delta H\#$ = 58.7 kJ mol-1 was calculated from the electrochemical results from 25 to 50°C. The main reaction pathway was quantifying by rotating ring-disk electrode (RRDE). The maximum amount of hydrogen peroxide produced in the ORR reaches a value of 3.8% at 0.36V/NHE following preferentially the four-electron transfer mechanisms to water formation. The current densities results revels that Pt catalysts with high activity and selective for the ORR can be obtained by the photo-deposition method.

Key words: Platinum electrocatalyst, photo-chemical, oxygen reduction, rotating disk electrode

1. Introduction

Proton exchange membrane fuel cells (PEMFC) has been receiving much attention as power sources for vehicles, portable devices and stationary applications due to their high energy conversion efficiencies and low pollutant emissions. The performance of a membrane electrode assembly for PEMFC greatly depends on the activity and loading amount of the electrocatalysts [1]. Platinum supported on high surface area carbon is still the catalyst most widely used in the fuel cell, this is for both electrodes: anode and cathode [2-3]. One of the major challenges in this field is the development of high-performance cathode catalysts in order to reduce the high overpotential present during the oxygen reduction reaction (ORR) [4-6]. The kinetics of oxygen reduction reaction is determined by various factors, which involve the geometric and electronic parameters of the material that catalyzes the reaction. One of the most important aspect in the ORR is the interaction of oxygen molecule with active sites of the catalyst, this is related with the catalytic activity, that is, with the size of its particles, its geometry and composition, its

dispersion and interaction with the support, it is important to control these factors during the synthesis process of the catalyst by means of an appropriate selection of the synthesis method [7-8].

Pt supported electrocatalysts for PEMFC normally are synthesized in the presence of a capping agent via reduction of a Pt precursor, decomposition of an organometallic complex, or a combination of these two routes [9-10]. However, in order to improve the metal dispersion, reduced the nanometer sizes and improve the interaction between the catalyst and the support, in the present work we prepared Pt nanoparticles with a homogeneous dispersion on carbon Vulcan using a photochemical route as synthesis method [11-16]. One of the advantages of this technique is the facile and low cost to synthesize nanometer platinum particles without thermal treatments with the possibility of employ both inorganic and organic precursors [17]. In this work, we report results concerning to the synthesis, physical characterization and electrochemical activity of the Pt/C catalyst for the ORR. Also, the mechanism of the catalyst activity toward water formation and the effect of temperature on the ORR kinetics for the Pt catalyst were investigated.

2. Experimental

2.1 Electrocatalysts preparation

10 wt.% Pt/C catalyst was synthesized by a photo-chemical method [16-17]. The platinum nanoparticles deposition onto the carbon Vulcan was carried out using a commercial photo-reactor (Luzchem Model LZV-4V) with 14 UV black light lamp of 20 W with the main wavelength at 365 nm. A platinum aqueous solution ($C_{10}H_{14}O_4Pt$ (Aldrich)) (5×10^{-4} M), prepared with an excess of ethanol (1:3), was bubbled with Nitrogen to remove the dissolved oxygen. Under this condition, the alcoholic solution was continuously stirred and irradiated for 3h. After this time irradiation, the quantity of Vulcan carbon necessary was added to obtain the 10 wt.% Pt/C catalyst. The resultant suspension was heated in an oven at 100 ºC overnight to remove the solvent by evaporation. The product obtained was a powder of the metallic platinum nanoparticles supported on carbon, labeled Pt/C-photo.

2.2 Physical characterization

The particle size distribution and the surface morphology of Pt/C-photo sample was obtained with Transmission Electron Microscopy technique (TEM) using a JEOL-JEM-2200 field emission operated at 200 kV. The dry samples obtained after the irradiation were prepared by dispersion in ethanol by ultrasound and the resulting suspension was deposited onto a copper mesh and dried at ambient conditions before TEM analysis.

X-ray diffraction (XRD) patterns of platinum catalyst were collected on a Bruker D8 AXS equipment using a Cu anode (K_α, λ=1.5406 Å) and a Bragg-Brentano configuration. The angle 2θ was varied between 20 to 100º with a stepwidth of 0.2° min^{-1} and 35 kV.

The H_2 chemisorption (pulse method) analysis was performed to determine the average active particle size and metal dispersion (it is defined like the relation between the number of Pt surface atoms and the number of Pt total

atoms).This analysis was carried out applying pulses of H_2 to the sample using an Autochem II 2920 equipment (Micromeritics) with a thermal conductivity detector (TCD) [16].

2.3. Electrochemical Characterization

Rotating disk electrode (RDE) and rotating ring-disk electrode (RRDE) techniques were employed to determine the activation energy and main reaction pathway, quantifying the amount of hydrogen peroxide produced during the oxygen reduction reaction. For RDE experiments, 8 µl of a sonicated mixture of 1mg of Pt catalyst, 60 µl of ethyl alcohol (spectrum grade) and 8µl of 5wt% Nafion® solution (Du Pont, 1000EW) were deposited on a glassy carbon electrode (GC) with a cross-sectional area of 0.19 cm^2.

For RRDE experiments, a commercial RRDE-PAR glassy carbon disk (diam=4.57 mm) and platinum ring with N=0.21 of nominal collection efficiency was used. The catalytic ink was prepared with 1mg of catalyst, 8 µl of 5 wt% Nafion® solution (Du Pont, 1100 EW), 100 µl of water and 100 µl of ethyl alcohol (spectrum grade). 8 µl of this suspension were deposited on the disk of working electrode surface. The current density was calculated using the geometric surface area.

The electrochemical measurements to RRDE were carried out at room temperature in a single, conventional, three-electrode test electrochemical cell. A platinum mesh was used as the counter electrode, and $Hg/Hg_2SO_4/0.5M\ H_2SO_4$ (MSE=0.680 V/NHE) as the reference electrode. RDE experiments were carried out in a water thermostated three-compartment cell for temperature control.The reference electrode was placed outside the cell, kept at room temperature and connected by a porcelain Luggin capillary. The temperature of the cell was controlled by a thermostat (Haake F3) from 293 to 323 K.

All experiments were performed in a Potentiostat AutoLab PGSTAT12 and a Pine MSRX rotation speed controller. A 0.5 M H_2SO_4 (Merck) aqueous solution was used as electrolyte, prepared from distilled water.The potentials in this paper are related to normal hydrogen electrode (NHE). Before the ORR measurements, cyclic voltammetry (CV) was performed from 0 to 1.2 V at 50 mV s^{-1} in an argon-saturated electrolyte, to clean the electrode surface. Ten cycles were necessary to stabilize the current–potential signal. Thereafter, the acid electrolyte was saturated with pure oxygen and maintained on the electrolyte surface during the RDE and RRDE tests. Hydrodynamic experiments were recorded in the rotation rate range of 100 to 1600 rpm at 5 mV s^{-1}. Between each measurement, the acid electrolyte was saturated with pure oxygen for 5 minutes to obtain the stable open circuit potential.

The experimental techniques selected for determination of Electrochemical Active Surface Area (EAS) were the cyclic voltammetry in in argon saturated 0.5 M H_2SO_4, at 50 mV s^{-1} by integrating the hydrogen-adsorption/desorption reaction (H_{upd}), Eq. (1), and the oxidation of adsorbed carbon monoxide or CO stripping technique. The electrode potential was held at 0.1 V/NHE and CO bubbled by 5 min. Thereafter, the CO was removed by purging the electrolyte with argon by 15 min and the test electrode swept from 0.05 V to 1.2 V/NHE until the post-CO oxidation was completed. Eq. (2):

$$EAS_{H\,upd} = \frac{Q_H}{0.210\,mC\,cm^{-2}} \quad (1)$$

$$EAS_{CO} = \frac{Q_{CO}}{0.420\,mC\,cm^{-2}} \quad (2)$$

where, Q_H and Q_{CO} are the measured charges for H_{upd}, and CO oxidation (mC), respectively. 0.21 mC cm^{-2} and 0.42 mC cm^{-2} corresponds to the charge required to oxidize a monolayer of adsorbed hydrogen and carbon monoxide species on Pt, respectively [18].

3. Results and discussion

3.1. Physical characterization results

Figure 1 shows the XRD diffraction patterns of Pt/C-photo sample. The powder electrocatalyst showed five diffraction peaks at 2θ values of 39.8º, 46.2º, 67.4º, 81.2º and 85.7º characteristics of the (111), (200), (220), (311) and (222) planes of face-centered cubic structure of platinum.

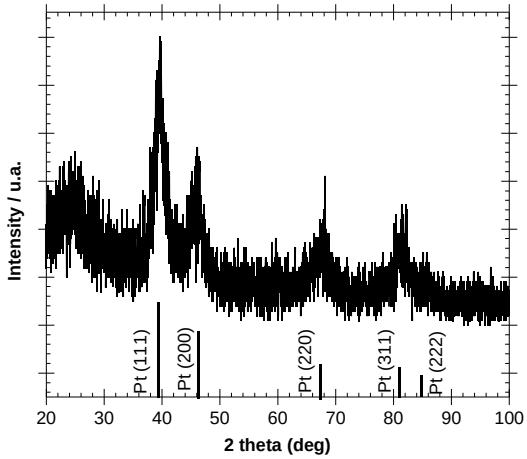

Figure 1. X ray diffraction patterns of Pt/C-photo catalyst synthesized by photo-deposition method.

TEM micrograph of platinum supported on carbon prepared by photo-deposition method is shown in figure 2. According to the figure 2, a homogenous distribution of Pt nanoparticles less than 5 nm onto de carbon was obtained. The average particle size and platinum dispersion on carbon support were investigated by H_2 chemisorption as complementary study.

Table 1. Physical and electrochemical parameters of Pt/C-photo sample.

Catalyst	*Average particle size (mn)	*Platinum dispersion (%)	EAS $_{CO}$(cm^2_{Pt})	EAS (H_{upd}) (cm^2_{Pt})
Pt/C-photo	5.2	21.5	5.5	5.01

*Estimated by H_2 chemisorption technique.

The results are reported in Table 1. Assuming spherical Pt particles, Pt/C-photo catalyst shows a small nanometer size (5.2 nm) with a platinum dispersion of 21.5 %. These results mean that the photo-chemical route allows preparing right Pt nanoparticles dispersed onto the carbon, by irradiation of the platinum acetil-acetonate precursor at room temperature.

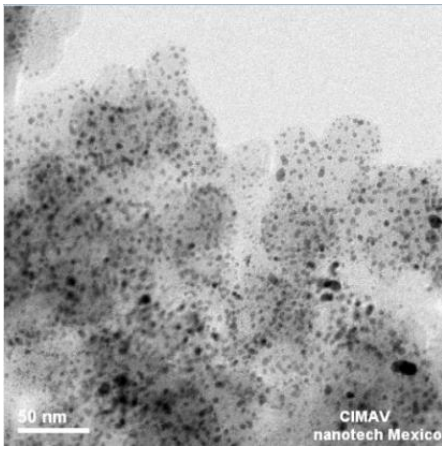

Figure 2. TEM graph for Pt/C-photo electrocatalysts synthesized by photo-deposition method.

3.2. Electrochemical characterization

Figure 3(a) shows a representative set of polarization curves for the ORR on the Pt/C-photo electrocatalyst in 0.5M H_2SO_4 at 318 K. Well defined kinetic currents (j_k) (0.93-0.83 V/NHE), mixed-diffusion limiting currents (0.83-0.60 V/NHE) and diffusion limiting currents (j_d) (0.2-0.6 NHE) are observed in polarization curves. It is considered that the increase in limiting currents on high performance electrocatalysts is associated with the increase of molecular oxygen diffusion in the boundary layer through the electrode surface. The reduction reaction is fast enough at high cathodic overpotentials, associated in almost all the cases to a flat limiting plateau. An explanation of the well defined catalytic current plateau of figure 3(a) could be associated to the existence of a uniform distribution of electrocatalytic sites on the electrode surfaces. When distribution of active sites is less uniform and the electrocatalytic reaction is slower, the current plateau is more tilted.

Table 2. Electro-kinetic parameters of Pt/C-photo electrocatalysts at different temperature.

Temperature K	**Slop Tafel mV dec^{-1}**	**Transfer coefficient α**	**Exchanger Current Density J_o mA cm^{-2}**
298	-82.10	0.72	1.30 x 10^{-6}
303	-82.48	0.73	1.55 x 10^{-6}
308	-81.78	0.74	1.81 x 10^{-6}
313	-81.17	0.76	3.03 x 10^{-6}
318	-80.78	0.79	5.60 x 10^{-6}
323	-79.28	0.80	7.17 x 10^{-6}

Figure 3(b) shows the mass transport corrected Tafel plots obtained for the Pt/C photo-electrocatalyst ink-type electrode on which oxygen reduction kinetics studies were conducted at different temperatures, from 293 to 323 K. The Tafel plots were obtained after the measured currents were corrected for diffusion to give the kinetic currents in the mixed activation–diffusion region, calculated from Eq. (3):

$$j_k = j\frac{j_d}{j_d - j} \tag{3}$$

Where $j_d/(j_d–j)$ is the mass transfer correction. The Tafel plots at all temperatures show a linear behavior in the mixed activation–diffusion region and a deviation of the kinetic current occurs with higher slope at high current density.

The kinetic parameters deduced for the oxygen reduction on Pt/C-Photo catalyst ink-type electrodes at different temperatures are presented in Table 2. The temperature analysis on the kinetic parameters is important in the cathodic reaction of a fuel cell. Effects such as the increase of the current and shift of the curves to more positive potentials were observed with the temperature rise. This behavior indicates an enhancement of the kinetic reduction of the adsorbed oxygen with the temperature. The dependence of the reversible oxygen electrode potential, E_r, on temperature [19] was evaluated using the value of ΔG° (H_2–O_2 cell) at each temperature using equations (4) and (5):

$$\Delta G^0 = \left[-70650 - 8T\ln T + 92.84T\right] \quad \text{cal mol}^{-1}, \tag{4}$$

$$E_r = -\Delta G^0 / nF \tag{5}$$

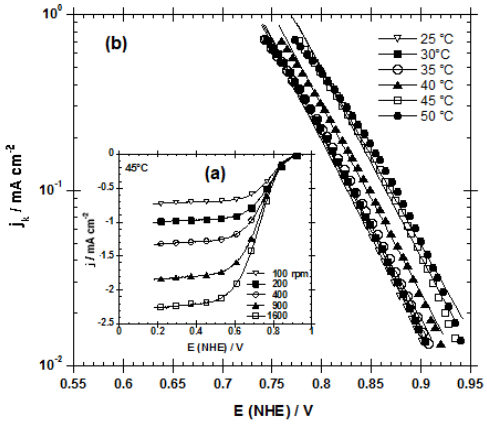

Figure 3. (a) Steady-state current-potential curves for ORR at different rotating speed, in oxygen saturated 0.5 M H_2SO_4 electrolyte at 5 mV s^{-1} and 45°C, (b) Mass-transfer corrected Tafel plots at different temperatures on Pt/C-photo electrocatalyst.

The temperature dependence of the exchange current density in Table 2 was analyzed via conventional Arrhenius analysis. Figure 4(a) shows an Arrhenius plot constructed for the Pt/C-Photo electrocatalyst in 0.5M H_2SO_4. The apparent enthalpy of activation, $\Delta H^{\#}$, was calculated from the linear regression analysis of the slope of the Arrhenius equation represented by the equation (6),

$$\frac{d\log j_o}{d(1/T)} = -\frac{\Delta H^{\#}}{2.303R} \tag{6}$$

An apparent enthalpy of activation $\Delta H^{\#}$ = 58.7 kJ mol^{-1} was calculated from the slope of this plots. This value is in agreement with apparent activation energies reported for platinum-base electrocatalysts for the ORR in acid media [20]. The apparent activation energy of 58.7 kJ mol^{-1} determined in 0.5M H_2SO_4 lies in the range of 25–60 kJ mol^{-1} reported for other materials for the oxygen reduction in acid media [19, 21]. One should keep in mind that the assessment of the activation energy at the reversible oxygen potential is only an estimate of the activation energy, i.e. $\Delta H^{\#}$ is the apparent activation energy.

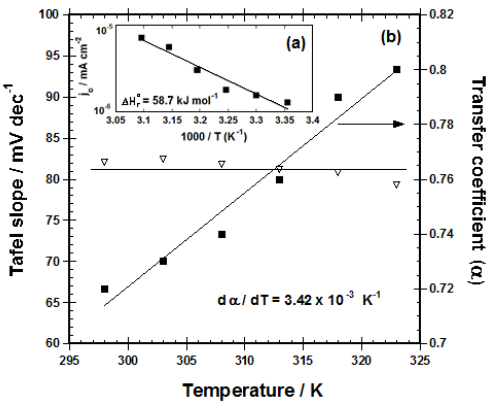

Figure 4. (a) Electrochemical Arrhenius plot of the exchange current density at the reversible potential for the ORR. (b) Variation of Tafel slope and transfer coefficient with temperature

The Tafel slope, *b*, is dependent on temperature according to the relation given by equation (7) [20]:

$$b = \frac{dE}{d\log i} = \frac{-2.303RT}{\alpha nF} \tag{7}$$

where: *n* and α are the number of electrons transferred and the transfer coefficient, respectively. Theoretically, *b* is temperature dependent if α is assumed to be invariant with temperature. Temperature dependence of the Tafel slope and transfer coefficient are shown in figure 4 (b). Here it can be observed that an experimental average Tafel slope of

-80 mV dec^{-1} is practically invariant with temperature for all the samples, leading to a dependence of the transfer coefficient with temperature. An increased linear variation of the charge transfer coefficient with respect to the absolute temperature ($d\alpha/dT$= 3.42 x10^{-3} K^{-1}) is also shown in figure 4. This behavior represents a significant feature and has been considered as an exception in the ORR rather than a rule in this electrochemical process [20-22]. In general the transfer coefficient α varies with the absolute temperature by the linear relationship, equation (8):

$$\alpha = \alpha_H + T\alpha_S \tag{8}$$

Where α_H is the enthalpic and α_S the entropic component to α.The term α_H is related to the change of electrochemical enthalpy of activation with electrode potential; mean while α_S is related to the change of electrochemical entropy of activation with electrode potential [23]. α_H and α_S were evaluated from the slope and interceptof a nominated Conway plot of the reciprocal of the Tafel slope against 1/T (plot not included) give the equation (8)

$$\alpha_{M1} = \alpha_H + T\alpha_S = -0.326 + 0.0035K^{-1}T \tag{9}$$

α_H is found to be -0.326 and α_S=3.5×10^{-3} K^{-1}. The value of α_H, suggests a less enthalpic contribution of the electrocatalyst to the ORR than entropy transfer coefficient (α_S). Thus, entropy transfer-coefficient is the determining factor for the catalytic activity of this reaction, indicating that the activation entropy turn over plays one of the most important roles in this cathodic electrochemical process.

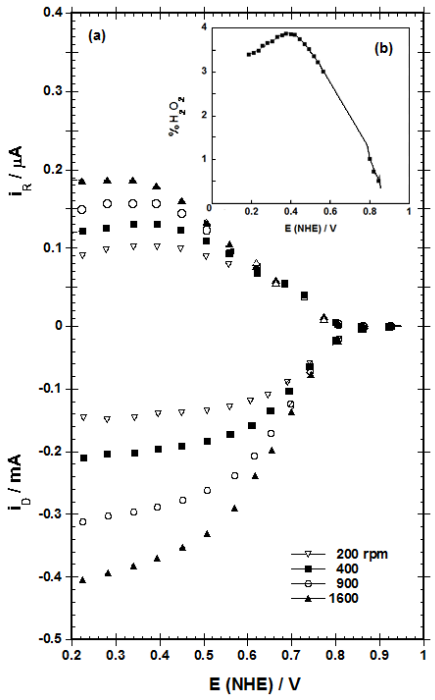

Figure 5. (a) Steady state polarization curves at different rotation speed as a function of disk potential for ORR in 0.5 M H_2SO_4 at 25 °C. (b) Percentage of hydrogen peroxide produced for the ORR.

The ORR is a complex reaction that proceeds via several consecutive and parallel elementary steps. It has been accepted that this occurs along two principal pathways: the first is the direct reduction to water with the transference of $4e^-$; the second is the so-called "peroxide pathway", which involves the transfer of $2e^-$ to the formation of H_2O_2 as intermediate. In this study, the RRDE technique was used in order to determine the amount of hydrogen peroxide produced [24]. The collection efficiency (N) was obtained experimentally from the slope of an i_R versus i_D plot at different rotation speeds, using as an electrolyte a $5x10^{-3}$ M $K_3Fe(CN)_6$ solution in 0.1 M K_2SO_4. A value of N = 0.16 for this arrangement was calculated on the thin film formed on the glassy carbon electrode. The ring potential was kept at +1.48V (NHE) during all of the electrochemical experiments, where oxidation of the H_2O_2 formed by O_2 reduction on the disk electrode is limited by diffusion.

Steady-state polarization curves obtained for the ORR in the disk and the currents for the hydrogen peroxide oxidation in the ring to Pt/C-Photo electrode are shown in Figure 5. In the oxygen saturated solution, the diffusion currents in the disk and ring are observed as a function of rotation speed. The peroxide percentage was evaluated from the following equation [25]:

$$\%H_2O_2 = \frac{200\ I_R/N}{I_D + I_R/N} \tag{10}$$

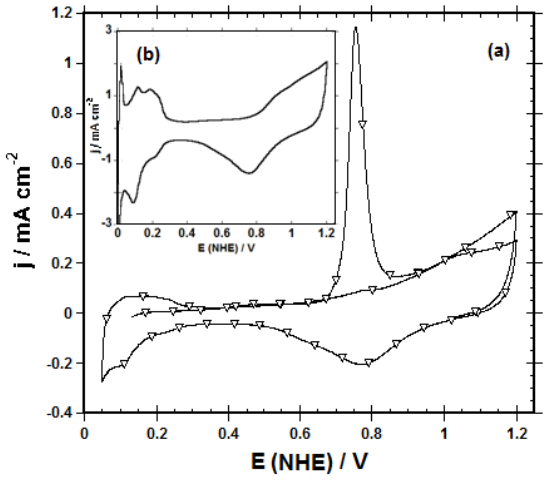

Figure 6. (a) Steady state polarization curves at different rotation speed as a function of disk potential for ORR in 0.5 M H_2SO_4 at 25 °C. (b) Percentage of hydrogen peroxide produced for the ORR.

Figure 5(b) shows that the quantity of hydrogen peroxide formation depends on the potential. The maximum amount of H_2O_2 produced in the electrochemical process of the ORR reaches a value of 3.8 % at 0.36 V/NHE on Pt/C-Photo electrode. The maximum amount of peroxide is preferable at more cathodic potentials because the fuel cell operates between 0.8 V (NHE) and 0.6 V (NHE).These results indicate that the Pt/C-Photo has a yield near 96.2 % for the

ORR (i.e., $\%H_2O = 100- \%H_2O_2$), following preferentially the four-electron transfer mechanisms to water formation. Figure 6 (a) shows the CO-stripping curves corresponding to electrocatalyst Pt/C-photo. Table 1 summarizes the electrochemical active area EAS (CO) obtained under the oxidation CO curve. In order to complement the results, the electrochemical active surface area (EAS) was calculated in hydrogen adsorption-desorption region (H_{upd}), figure 6 (b). The H_{upd} charge is estimated for hydrogen adsorption/desorption in the CV profile after the conventional correction for the pseudocapacity in the double layer region. Similar EAS were found by both techniques, CO stripping and Hupd. The EAS depends of the particle size, distribution and quantity of surface particles. In this case, the real surface area differs highly from the geometric one, indicating high catalytic activity. The electrocatalysis mechanism is based on the electrode–electroactive species charge transfer through the electrode surface. So the reaction rate, and consequently the electric current, is proportional to the electrode real surface area [26].

4. Conclusions

Pt nanoparticles can be prepared at room temperature by the photo-deposition method. The physical characterization of the synthesized platinum showed a homogeneous distribution of platinum nanoparticles onto the carbon with an average particle size of 5 nm. Pt/C electrocatalyst showed activity and selectivity towards the ORR process in acid medium. The ORR followed preferentially the four-electron transfer mechanism to water formation. The effect of temperature on electrochemical parameters showed that the Tafel slope is directly proportional to the temperature with the transfer coefficient a temperature-independent factor.

Acknowledgements

This work has been supported by the IPN under project SIP-20113593 and CONACYT project 130254. BRC thanks PIFI and CONACyT programs for the financial support (scolarship).

References

[1] B. Zhang, L.J. Chen, K.Y. GE, Y.C. Gou, B.X. Peng, Chinese Chemical Letters, 16, 1531-1534 (2005).

[2] E. Antolini, Appl. Catal. B, 88, 1-24 (2009).

[3] L.G.R.A. Santos, K.S. Freitas, E. A. Ticianelli, J. Solid Stated Electrochem 11, 1541-1548 (2007).

[4] J.J. Salvador-Pascual, S. Citalán-Cigarroa, O. Solorza-Feria, J. PowerSources, 172. 229-234 (2007).

[5]S. Chen, P.J. Ferreira, W. Sheng, N. Yabuuchi, L.F. Allard, Y. Shao-Horn, J. Am. Chem. Soc. 130, 12818-13819 (2008).

[6] L. Zhang, J. Zhang, D.P. Wilkinson, H. Wang, J. Power Sources 156, 171-182 (2006).

[7] B. Ruiz Camacho, M. Torres Rodríguez, O. Solorza Feria, J. New Mat. Electrochem.Syst. 12, 043-047 (2009).

[8] S. Zhang, X.-Z. Yuan, J.Z. Cheng Hin, H. Wang, K. A. Friedrich, M. Shulze. J. Power Sources 194, 588-600 (2009).

[9]John Regalbuto, "Catalyst Preparation Science and Engineering", CRC Press, Taylor and Francis Group, New York, 2007.

[10] J. Chen, B. Lim, E.P. Lee, Y. Xia, Nano Today 4, 81-95 (2009).

[11] H. Einaga, M. Harada, Langmuir 21, 2578-2584 (2005).

[12] L. Timperman, Y.J. Feng, W. Vogel, N. Alonso-Vante, Electrochim. Acta 55 7558-7563 (2010)

[13] K. Rajeshwar, N. R. de Tacconi, C. R. Chenthamarakshan, W. A. Wampler, T. Carlson, and W.-Y. Lin, U.S. Patent, pending.

[14] N. R. Tacconi, C.R. Chenthamarakshan, K. Rajeshwar, W.-Y. Lin, T.f. Carlson, L. Nikiel, W.A. Wampler, S. Sambandam, W. Ramani, J. Electrochem. Soc. 155 B1102-B1109 (2008).

[15] C. Crisafulli, S. Scire, S. Giuffrida, G Ventimiglia, R. Nigro, Appl. Catal. A, 306, 51-57 (2006).

[16] B. Ruiz Camacho, M.A. Valenzuela, J.A. Perez Galindo, F. Pola, M. Miki-Yoshida, N. Alonso-Vante, R. G. González Huerta, J. New Mat. Electrochem. Syst. 13, 183-189 (2010).

[17] Ruiz Camacho, R. G. González Huerta, M. A. Valenzuela, N. Alonso-Vante, Top. Catal. 54, 512-518 (2011).

[18] T. Vidakovic, M. Christov, K. Sundmacher, Electrochim. Acta 52, 5606-5613 (2007).

[19] K. Suárez-Alcántara, A. Rodríguez-Castellanos, R. Dante, O. Solorza-Feria, J. Power Sources 157, 114–120 (2006).

[20] R. G. Gonzalez-Huerta, A. R. Pierna and O. Solorza-Feria, J. New Mat. Electrochem. Syst. 11, 63-67 (2008).

[21] J.J. Salvador-Pascual, V. Collins-Martínez, A. López-Ortíz, O. Solorza-Feria, J. Power Sources 195, 3374–3379 (2010).

[22] V. S. Murthi, R. C. Urian, and S. Mukerjee, J. Phys. Chem. B 108, 11011-11023 (2004).

[23] A. Damjanovic, J. Electroanal. Chem. 355, 57-77 (1993).

[24] G. Ramos-Sánchez, A.R. Pierna, O. Solorza-Feria, Journal of Non-Crystalline Solids 354, 5165–5168 (2008).

[25] U.A. Paulus, T.J. Schmidt, H.A. Gasteiger, R.J. Behm, J. Electroanal. Chem. 495, 134-145 (2001).

[26] José M. Doña Rodríguez,* José Alberto Herrera Melián, Jesus Pérez Peña, J. Chem. Edu., Vol. 77 No. 9, 1195-1197 (2000).